Establishment of an Integrated Italy–Malta Cross–Border System of Civil Protection. Geophysical Aspects
ISBN 978-88-548-8256-0
DOI 10.4399/97888548825607
pag. 79–98 (october 2015)

v. Evaluation of seismic site response in the Maltese archipelago

Farrugia D., Paolucci E., D'Amico S., Galea P., Pace S., Panzera F., Lombardo G., and INGV team[1]

1. Introduction

The investigation of local ground conditions is an important part of seismic hazard assessment (Fäh *et al.*, 2003). It is now well–established that earthquake ground shaking is not only a function of the earthquake magnitude and epicentral distance, but also of the site conditions, including soft layers in the sub–soil stratification and topographical features. Local geology can greatly alter the seismic waves from earthquakes by amplifying their amplitude, changing the frequency content and increasing the shaking duration during an earthquake (Kramer, 1996). In fact, several unconsolidated soft sites have suffered significantly greater damage than rock sites. One case was the 1985 Michoacán earthquake which showed low peak ground acceleration near the epicenter, yet caused severe damage in Mexico City, which is found more than 350 km away and is characterized by soft shallow sediments (Campillo *et al.*, 1989).

The main parameters responsible for such effects are the shear–wave velocity (V_S) structure and thickness of the sedimentary cover, the impedance contrast between the soft sediments and the underlying bedrock as well as the geometry of their interface (Parolai *et al.*,2006). Knowledge of the V_S structure and/or the resonance frequency of soft soil layers is of utmost importance for the prevention or mitigation of earthquake disasters (Arai and Tokimatsu, 2005). Such information should contribute to earthquake–hazard mitiga-

1. Pischiutta M., Villani F., Vassallo M., Amoroso S., Cantore L., Di Naccio D., Mercuri A., Rovelli A., Famiani D., Cara F., Di Giulio G., Akinci A.

tion strategies such as seismic risk assessments, emergency response–preparedness and land use planning by considering existing and proposed buildings (Zor *et al.*, 2010).

Various techniques have been developed so that this data can be acquired, such as borehole logging and penetrometry. Although they provide the most direct measurements, these invasive techniques suffer from limitations which include the use of relatively expensive equipment and the difficulty in conducting measurements in urbanized areas due to the drilling involved. Because of their cost, these techniques are usually limited in exploration depth. In fact, the average V_S in the upper 30 m (V_{S30}) is used for microzonation purposes and is adopted by several seismic design and building codes to evaluate potential site amplifications (Zor *et al.*, 2010, Picozzi *et al.*, 2009). Other techniques use real earthquake data to measure directly the site response, however these can only be successful in areas characterized by a high seismicity (Bonnefoy–Claudet *et al.*, 2006).

During the past few decades, passive techniques which make use of ambient noise (or microtremors) have been developed and are becoming increasingly popular, owing to a number of advantages. These techniques are convenient since they provide quick reliable estimates with good lateral coverage, utilizing relatively cheap equipment which can be installed in urban areas (Parolai *et al.*, 2005).

Ambient noise techniques rely on the assumption that fundamental mode surface (Rayleigh and Love) waves dominate the noise wave–field. This argument is still being debated in the geophysics community as this dominance depends on various factors such as the sources and the site itself (Bonnefoy–Claudet *et al.*, 2006). Notwithstanding this theoretical disagreement, studies, in general, have yielded results using ambient noise techniques which agree with those obtained from down– or cross–hole techniques (Parolai *et al.*, 2005).

In 2001, a detailed study on the reliability of low cost ambient noise techniques was conducted in a project named SESAME (Site Effect Assessment Using Ambient Excitation) (SESAME, 2004). The study focused on two main techniques: the single station H/V and the array method.

The H/V technique, first proposed by Nogoshi and Igarashi (1970) and later revised by Nakamura (1989), is a tool to estimate the resonance frequency of a soil deposit, f_0, which is related to the average shear–wave velocity $<V_S>$ and thickness H of a sedimentary cover by

the equation:

$$f_0 = \frac{\langle V_s \rangle}{4H} \quad (1)$$

Array techniques were originally developed during the 1950–1970s to detect and localize nuclear explosions. They were then adapted to derive the velocity of surface waves based on the simultaneous recordings at different locations. The geophones/sensors used in array techniques are mostly vertical component ones and so only the Rayleigh waves are recorded. Recently, however, some studies (e.g., Kohler *et al.*, 2007) are making use of 3–component sensors and thus include both Rayleigh and Love waves in their measurements.

As the name implies, surface waves travel close to a free surface and only affect a limited depth depending on their wavelength (Socco and Strobbia, 2004). The phase and group velocities of surface waves depend on the properties of the media that they propagate in, especially the V_S and the thickness of the layers, making them suitable for obtaining information on the subsoil structure at a site (Chavez–Garcia *et al.*, 2006). Array techniques rely on one important characteristic of surface waves — they are dispersive i.e. in vertically heterogeneous media their velocity varies with the frequency. The high frequency (short wavelength) Rayleigh waves propagate in the shallow part of

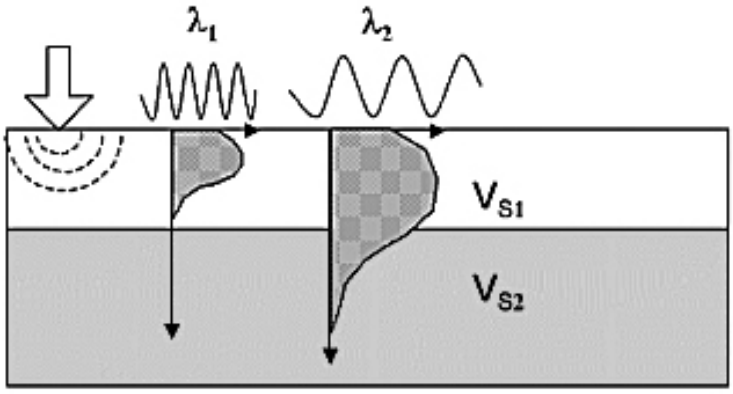

Figure 1. Geometric dispersion of Rayleigh waves: the shorter wavelength penetrates the shallow part while the longer wavelength penetrates the deeper part of the subsurface (Foti *et al.*, 2011).

the subsurface and are affected by the properties of the shallow layers, while the low frequency (long wavelength) ones penetrate to deeper regions (refer to Fig. 1).

Fig. 2 shows the main steps involved in surface wave techniques. After acquisition of some minutes of ambient noise, the data is first processed to obtain a dispersion curve (Rayleigh wave velocity vs. frequency). This is then inverted so as to obtain the shear–wave velocity profile.

Different surface wave processing methods have been developed during the past decades, the main ones being the Spatial Auto–Correlation (SPAC) method (Aki, 1957) and the frequency–wavenumber (f–k) analysis (Capon, 1969), which will be used in this project.

Various studies have shown that the local V_S profile can be obtained with good accuracy using surface–wave methods (e.g., Kuo *et al.*, 2009, Bettig *et al.*, 2001, Chavez–Garcia *et al.*, 2006, Scherbaum *et al.*, 2003) in particular when *a priori* information about the thickness of

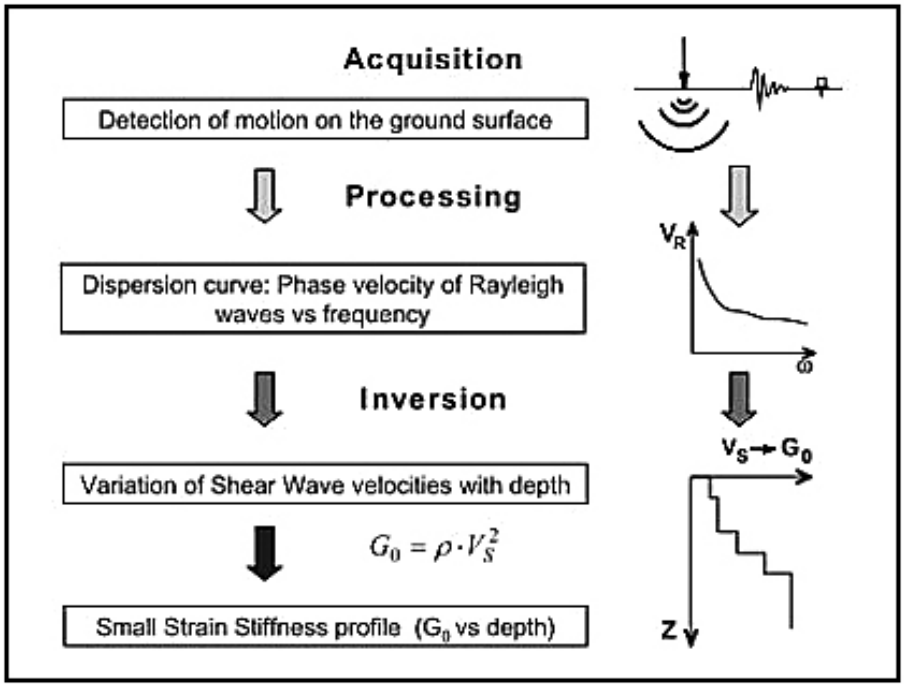

Figure 2. The steps involved in surface wave techniques (Foti *et al.*, 2011).

sedimentary cover is available from other geotechnical studies (Picozzi *et al.*, 2009).

1.1. *Overview of this study*

This report is divided into two parts. The results in the first part describe the correlation of the frequency/amplification characteristics, obtained using the H/V method, as a function of the geology over the Maltese islands. This was done to identify areas that could be more vulnerable than others, as well as to produce a map of the site response characteristics, and carry out some validation procedures in order to identify the origin of the amplification. Results from two densely studied sites are also presented.

In addition, a preliminary study at a site characterised by the clay layer was carried out using both array methods and H/V. The aim is to obtain a V_S profile of the site and an estimation of the V_S of the different stratigraphic layers while identifying the capabilities and limitations of the different techniques so that further studies at more complicated sites could be carried out.

Furthermore, in order to take the subsoil response into account in the hazard assessment of the Maltese islands, on November 2014 a scientific team composed by Istituto Nazionale di Geofisica e Vulcanologia (INGV), University of Malta and University of Catania researchers performed several geophysical investigations. These prospections included seismic and electrical 2D–tomography, MASW profiles, 2D arrays and single–station measurements using ambient noise. The final goal was to combine different geophysical methods which allow the reconstruction of geometries at depth (tens of meters) and the evaluation of shear–wave velocities in the most common geological formations outcropping on the islands. In each investigated site different experiments depending on site–specific geological and logistic conditions were carried out (more details in Pischiutta *et al.*, 2015). Special care was devoted to determine the thickness of the Blue Clay formation through electrical resistivity tomography (ERT). The inversion of apparent resistivity data acquired with a Wenner configuration of quadrupoles indicate that the thickness of the Blue Clay Fm may exceed 40 m.

2. Geology of the Maltese islands

The geology of the Maltese islands is relatively young, with the oldest rock dating back only to the Tertiary period. The islands are mostly composed of marine sedimentary rocks (Fig. 3). Although the sedimentary platform on which the Maltese islands are situated was formed during the Triassic, there are no surface outcrops of this age. All exposed rocks were deposited during the Oligocene and Miocene when the Maltese islands were part of the Malta–Ragusa platform with Sicily and, as such, attached to the African margin (Pedley *et al.*, 1978; Mourik *et al.*, 2011). The most recent deposits are the Quaternary deposits, which are found in minor quantities and are of terrestrial origin.

The geologic sequence of the Maltese islands is classically divided into five units (Pedley *et al.*, 1978, 2002). The lowermost and oldest unit is the Lower Coralline Limestone Formation (LCL), which consists of massive biogenic limestone beds of shallow gulf marine origin. This shallow carbonate ramp phase is Oligocene in age. Younger beds show evidence of deposition in more open marine conditions. Deeper water slope carbonates of the Globigerina Limestone Formation (GL) began depositing in the Chattian (Late Oligocene) and span from the early Miocene to late middle Miocene. They consist mainly of loosely aggregated planktonic foraminifers, whereas larger skeletal fragments, such as echinoids or mollusks, are rare. A marly unit of alternating light to dark layers, called the Blue Clay Formation (BC), spanning the Serravalian (middle Miocene) (Kienel *et al.*, 1995; Jacobs *et al.*, 1996), abruptly follows the GL. Planktonic and benthic foraminifers form the bulk of the skeletal components within this unit.

The water depth at which BC was formed is estimated on the basis of benthic foraminifers to be 150–200 m (Jacobs *et al.*, 1996), or even 500 m (Foresi *et al.*, 2002). The BC formation is unconformably overlain by the Greensand Formation (GS) and the Upper Coralline Limestone Formation (UCL), both late Miocene in age. The GS formation consists of a glauconitic sand bed ranging from 0 to 10 m in thickness, while the UCL consists of white porous calcareous sandstone, always rich in organic remains. Though some layers are completely crystalline and have lost traces of the organisms from which they originated, other portions are highly fossiliferous containing casts of

shells and other organisms. It resembles the LCL both on chemical and paleontological grounds, indicating deposition in shallow-water carbonate ramp conditions.

As can be seen from Figure 3, the eastern half of Malta is characterised only by the LCL and GL, giving rise to a flat, rolling landscape in this part of the islands. On the other hand, the western half of Malta and some areas in Gozo retain the full sedimentary sequence (Pedley *et al.*, 2002), with UCL hillcaps and plateaus overtopping BC gentle slopes being the dominant feature in the landscape of north–western Malta and north–eastern Gozo (Gigli *et al.*, 2012). In terms of V_S, the buried soft BC layer introduces a velocity inversion in the stratigraphy.

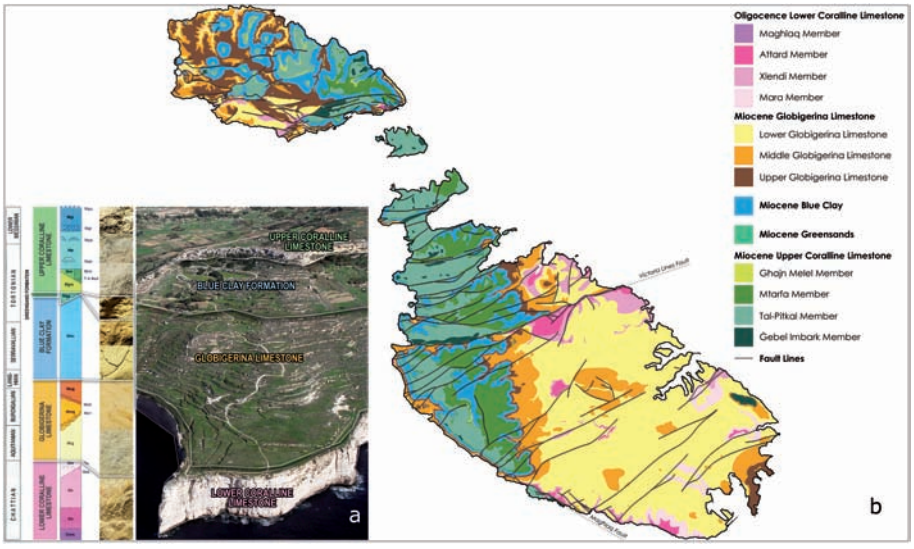

Figure 3. (a) The geological stratification of the Maltese islands including the members, sublayers, geological era, texture and outcrop occurrence of all the layers. The colour code is followed in subsequent figures (modified from The Geological Map of the Maltese Islands (Oil Exploration Directorate, Office of the Prime Minister, Malta, 1993)); and (b) outcrop geology of Malta and Gozo (Oil Exploration Directorate, Office of the Prime Minister, Malta, 1993) with topography and major fault patterns (Mapping Unit, Malta Environment and Planning Authority, MEPA, 2010). (Fig. from Vella *et al.*, 2013).

3. Data collection and results

Data were collected using Tromino 3–component seismographs (www.tromino.eu), which are compact, self–contained and highly portable instruments, and the Micromed SoilSpy Rosina™ equipped with 4.5 Hz geophones was used for array measurements. Processing was done via the Grilla™ and Geopsy software as well as software combining ESAC and Genetic Algorithm (GA) (Picozzi and Albarello, 2007).

3.1. *H/V results from single–station measurements*

During the past years, several H/V measurements were conducted in different studies (eg. Pace *et al.*, 2011, Vella *et al.*, 2013) around all the Maltese islands. Some of the results previously obtained are displayed in Figure 4. It can be clearly seen that there is a clear correlation between outcrop geology and site frequency response.

Fig. 5 shows typical H/V curves on different geological outcrops. The Lower Coralline and Globigerina Limestone sites exhibit mainly flat response curves above 0.5 Hz, the main range of engineering interest for typical local structures (Fig. 5d) (Vella *et al.*, 2013).

The effect of the Blue Clay layer, whether outcropping at surface, or as a buried layer beneath the hard Upper Coralline Limestone layer, is clearly evident in all the obtained H/V curves. The curves obtained on BC outcrop are characterised by pronounced and well–defined peaks in the 2–10 Hz range (Fig. 5c).

The variation in characteristic peak frequency due to the outcropping BC is attributed to the variation in the layer thickness. On the UCL, all the curves exhibit a peak between the narrow range of 1–2 Hz. This resonance can be interpreted as being due to the buried clay layer, however due to this narrow range the depth and thickness of the clay layer do not seem to play an important role in the peak frequency. The presence of the Blue Clay layer gives rise to a velocity inversion. This feature causes the H/V values to drop below 1 over a wide frequency range (Castellaro and Mulargia, 2009) as is evident in several cases.

In this study two further test sites have been investigated in more detail: the Xemxija Bay area (Pace, 2012) and Fort Chambray (Pace, 2015). They are located on the islands of Malta and Gozo respectively. The urban area of Xemxija on the NE coast of Malta is subject to

intensive touristic and recreational activities in the summer season. It has a complex geology and geomorphological structure, including a hilltop area, valley and coastal region. All the major geological layers can be found in Xemxija, with some area in the downthrown Pwales valley being covered by thick soil. The Pwales Valley is an area highly exploited for agricultural activities. It forms part of an extensive block faulting system that affects the northern part of the Maltese islands (Illies, 1981; Reuther and Eisbacher, 1985). The Pwales valley itself is a graben, defined by two faults within the horst–and–graben system, characterised by a sequence of ENE striking normal faults (MEPA, 2004).

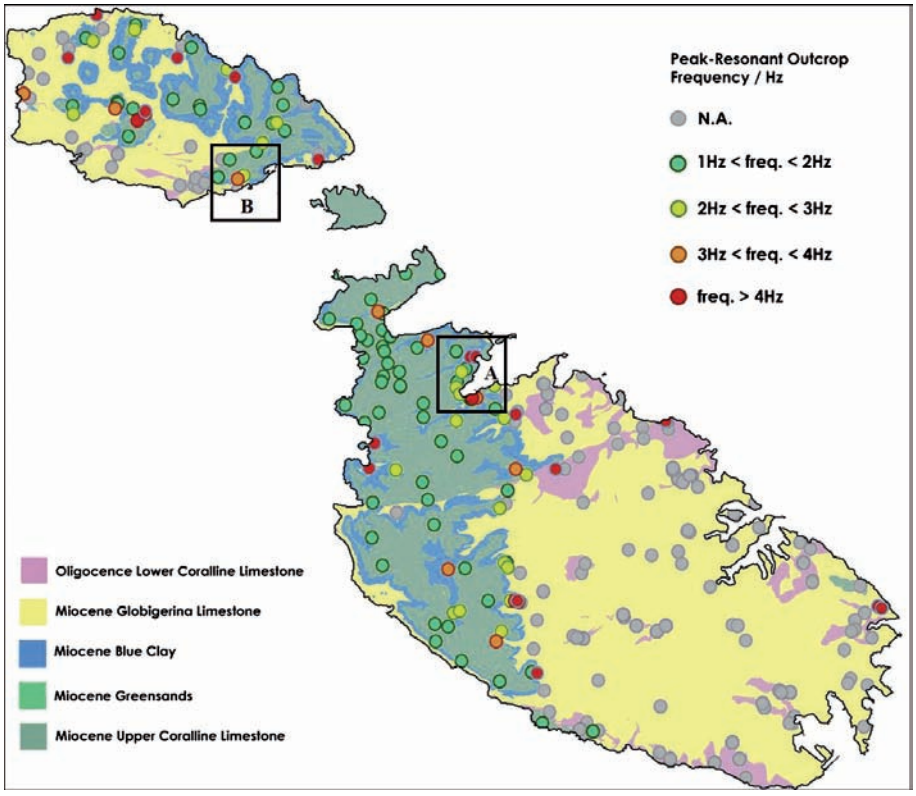

Figure 4. Site resonance frequency map for the Maltese islands. NA means "No amplification". The results shown are from a first, nation-wide H/V survey (Vella et al, 2013). More detailed microzonation studies were carried out in the areas shown by squares on the map (A = Xemxija area, B = Fort Chambray).

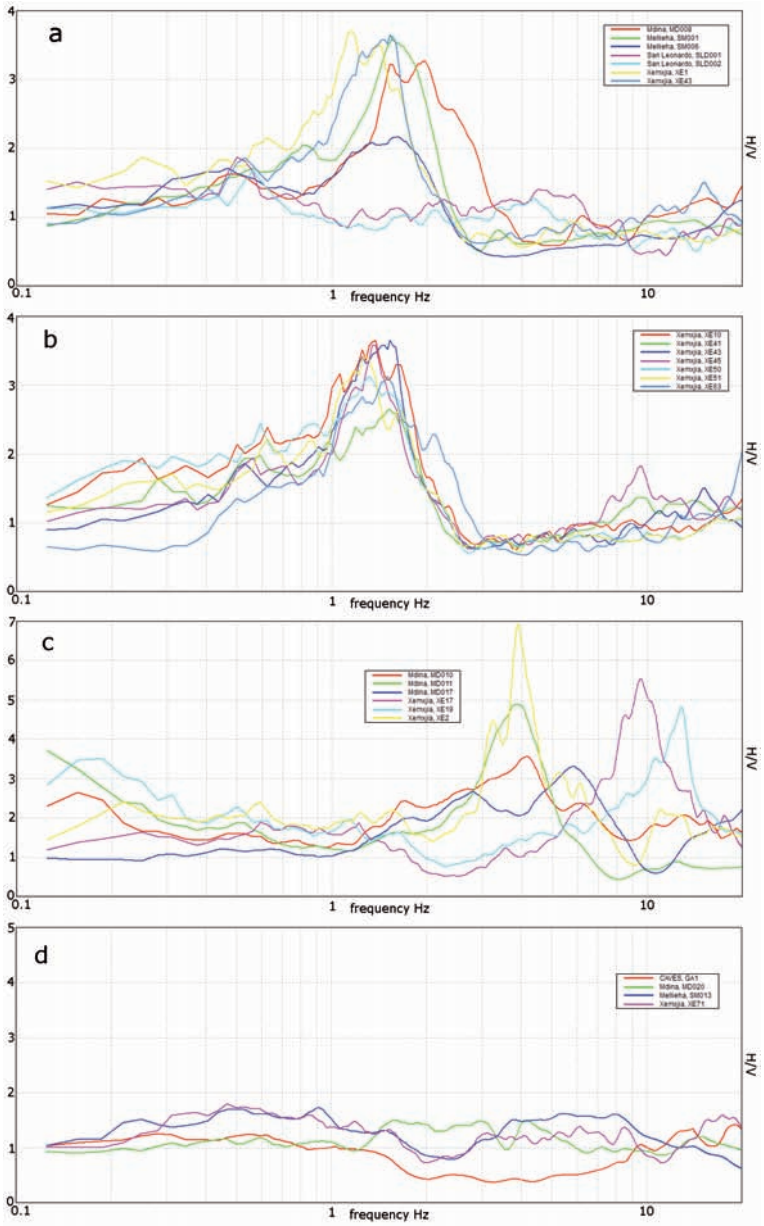

Figure 5. Examples of H/V curves obtained in different locations. (a) Sites on Upper Coralline Limestone. Note that the two curves that show no amplification were obtained from the only site in Malta where Upper Coralline Limestone is not underlain by Blue Clay (San Leonardo); (b) sites on Upper Coralline Limestone in one locality, Xemxija; (c) sites on Blue Clay; (d) sites on Lower Coralline Limestone and Globigerina Limestone (Vella *et al.*, 2013).

Pace (2012) conducted a dense microtremor measurement survey in Xemxija, with about 100 microtremor recordings performed at random positions, as well as along predetermined profiles. Fundamental frequencies obtained from measurements performed in the valley varied between 2.0 Hz to over 11.0 Hz (Fig. 6). This large spread is interpreted to be due to the different soil thicknesses above the UCL. These curves contrast with those obtained on the neighbouring hilltop, where no or negligible soil is present, as the frequencies obtained here vary between 1.0 and 2.0 Hz, just as was shown above (Pace, 2012).

At Fort Chambray, Gozo, (Fig. 7) a similar study was conducted and the results show that the peak on the UCL formation occurs at around 1.4 Hz whereas the fundamental frequency on BC ranges between 2.0 and 10.0 Hz.

3.2. *Shear–wave velocity profiles from array and H/V measurements*

Three different array techniques were first tested in a field situated in Fiddien, Rabat which is characterized by a layer of the soft Blue Clay

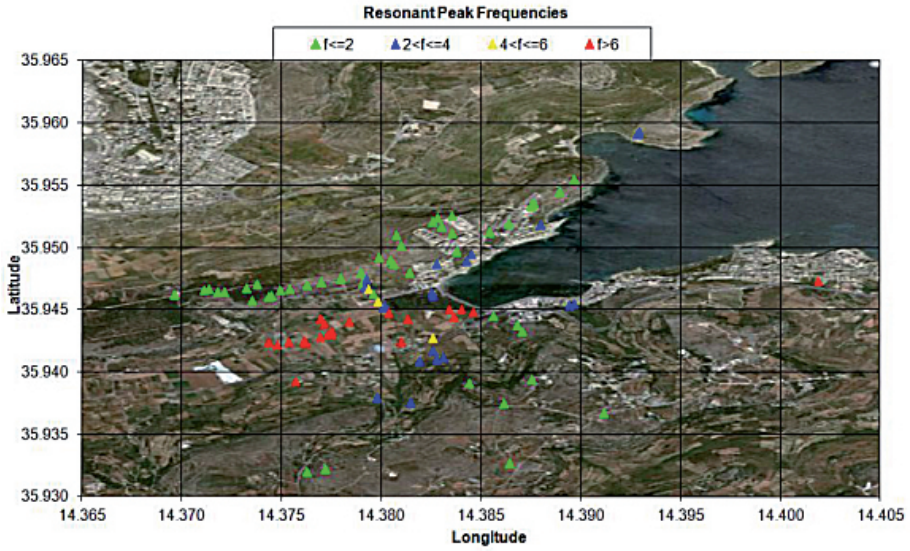

Figure 6. Resonant peak frequencies obtained in the Xemxija area (Malta) (Pace, 2012).

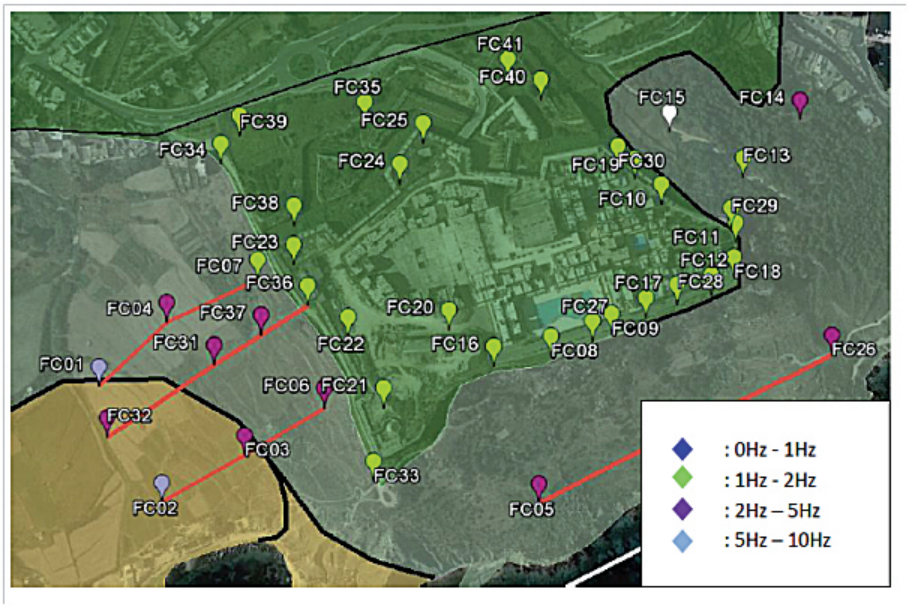

Figure 7. Resonant peak frequencies obtained in the Fort Chambray area (Gozo) (Pace, 2015).

(BC) overlying the harder Globigerina Limestone (GL). This site was chosen since it presents the ideal geology for such studies: a velocity profile in which V_S increases with depth.

The aim was to test and compare the capabilities and limitations of the three techniques which are: the Modified Spatial Auto–Correlation (MSPAC), Extended Spatial Auto–Correlation (ESAC) and *f–k* method. The results from three different array configurations were also compared. Specifically, the geometries are: an array of 17 geophones arranged in an L–shape and circle respectively (henceforth also referred to as short arrays) and 42 geophones in an L–shaped configuration (referred to as long array). The distance between consecutive geophones was around 5 m (limited by the cabling set-up). The chosen configuration ensured a good resolution of both shallow layers (due to the 5 m spacing) and deeper layers (since the long array had dimensions of 125 m and 80 m).

A series of 3–component single–station measurements were also carried out to obtain the H/V curve. This was then jointly inverted with the dispersion curve to infer the V_S profile of the site. Two dif-

ferent inversion algorithms, the Neighbourhood Algorithm (NA) and the Genetic Algorithm (GA), will be used and their results compared.

MSPAC analysis and inversion using the NA was conducted using the Geopsy software package, while the ESAC procedure and GA inversion was performed as in Albarello *et al.*, (2011).

3.2.1. Single–station (H/V) results

The results from the H/V survey was carried out in the field are displayed in Figure 8. The curves exhibit a consistent peak at around 2.0 Hz. In addition, some curves also exhibit secondary peaks (of lesser amplitude) which could be due to other impedance contrasts close to the surface (Picozzi *et al.*, 2009). This situation is likely because the BC is itself often layered due to weathering processes.

Since from previous studies it is known that the peak frequency of the H/V curve is representative of the depth to bedrock (refer to equation (1)), a consistent peak frequency in different points around the field is indicative of a constant thickness of clay. Thus the layers can be assumed to be horizontal, fulfilling one of the assumptions of array techniques i.e. the array should sample the same geology. It is important to verify this before taking any array measurements.

3.2.2. Array results

Fig. 9 shows the dispersion curves obtained using the ESAC and MSPAC technique for the three array configurations. In general, there is a good agreement between the curves. Some differences can be observed for the short and long L–shaped arrays (Figs. 9a and 9c respectively) in the lower frequency part of the curve with the MSPAC slightly underestimating the velocity. The two dispersion curves obtained for the circular array (Fig. 9b) differ slightly in the frequency band.

While the MSPAC provided results down to approximately 3.5 Hz, the ESAC curve contributed to the higher frequency part and goes up to 16 Hz. Since the MSPAC curve was manually picked, these slight differences in the curves could be related to the manual picking, which can be subjective at times.

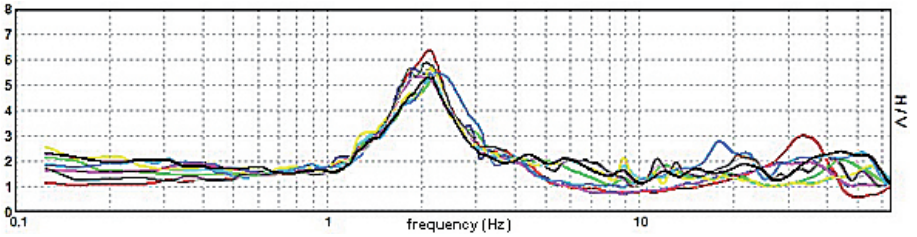

Figure 8. The H/V curves obtained at different points in the Rabat field.

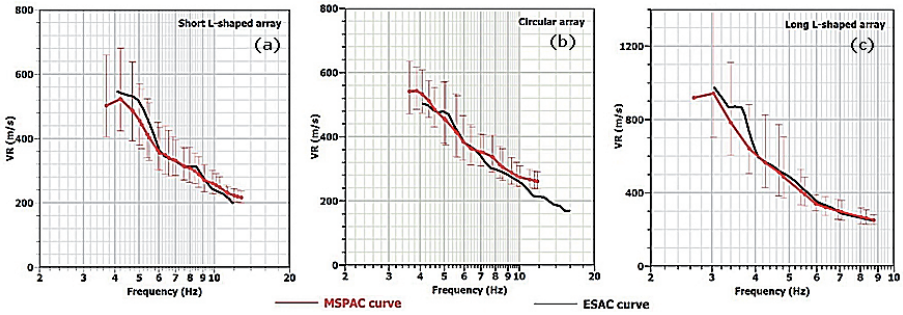

Figure 9. A comparison between the curves obtained using the ESAC and MSPAC methods, for each of the three array set-ups. The red curve represents the MSPAC curve while the black one corresponds to the ESAC curve.

In Figure 10, the MSPAC curves are compared to the curves obtained using the *f–k* processing technique (only the MSPAC curves were compared due to the similarity between the MSPAC and ESAC curves). It is reported in literature (Zor *et al.*, 2010, Picozzi *et al.*, 2009) that the *f–k* method has the tendency to overestimate the velocity at lower frequencies. This can be clearly seen in all the three curves in Figure 10. One other observation which can be made is that the error bars of both curves increase with decreasing frequency. This is a result of the limiting aperture of the array which increases the uncertainty in the deeper part of the subsurface structure (and thus in the low frequency part of the dispersion curve).

It is also important to test that the L–shaped array geometry is as equally valid as the circular one. Although some studies (Ohori *et al.*, 2002, Parolai *et al.*, 2006) have utilised the latter and achieved good results, other authors still criticise this type of configuration which

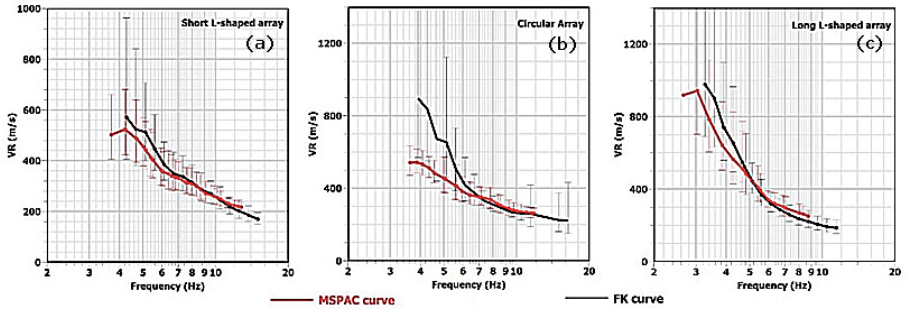

Figure 10. A comparison between the curves obtained using the *f–k* and MSPAC methods, for each of the three array set–ups. The red curve represents the MSPAC curve while the black one corresponds to the *f–k* curve.

lacks azimuthal coverage. Using an L–shaped array rather than just a single line of geophones is still an improvement as one has to be very careful when using one–dimensional arrays.

In general the characteristics and direction of the ambient wave–field are not known. It is normally assumed that the sources of ambient noise are distributed randomly. In this case, and given that the array output should be the same for all azimuths, a circular or quasi-circular array is usually considered to be the best configuration for azimuthal coverage. However this is not always possible, especially in urban areas where the buildings present make it difficult to achieve such a configuration. In this case, the geophones are connected by a cable, which sets a limit on the spacing of the geophones. The available GPS instrument has the accuracy of ±15 m, which is too large compared to the geophone spacing, and would thus give unacceptably large errors. Setting up the "perfect" circular array used in this field experiment required laborious work which goes beyond the scope of these techniques i.e. obtaining information in a quick way. It was therefore decided to use two–dimensional linear arrays in which the geophone positions could be accurately measured. The validity of the L–shaped array was thus tested by comparing the outputs of the two configurations.

As can be seen in Figure 11a, both arrays gave similar results. This justifies the use of the L–shaped array in the ensuing experiments. Such arrays can be set up much more easily and accurately with the available equipment.

Finally, Figure 11b, shows the MSPAC curves obtained when using the short L–shaped array and the longer one. As expected, a difference in the low frequencies can be observed. While the lowest observable frequency using the short array was around 4.0 Hz, this went down to 3.0 Hz with the larger array. It is important to note that in this case, apart from the array length, the resonance frequency of the geophones, i.e 4.5 Hz, also presents a limitation to the lower part of the frequency range.

From the above results, one can make an estimation of the maximum retrievable depth by looking at the attained wavelengths. The maximum wavelength from the MSPAC dispersion curve using the short L–shaped and circular array were 117 m and 137 m respectively while the larger array provided wavelengths up to 345 m. Assuming the maximum depth of investigation to be between 1/3 and 1/2 of the maximum wavelength obtained (Tokimatsu, 1997), the smaller array would approximately allow us to sample a depth of 40–65 m while the larger array allows to reach depths of 115-172.5 m. However, one must also consider that the soft layers act as a high pass filter (Scherbaum *et al.*, 2003) so that it could be difficult to get a reliable solution at these depths. In fact, the frequency range of each dispersion curve obtained was higher than the peak H/V frequency, which suggests that the

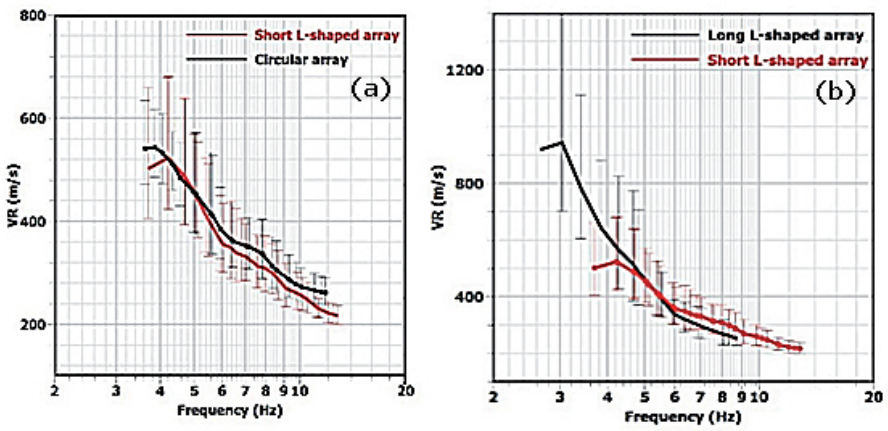

Figure 11. (a) A comparison of the MSPAC curve obtained from the short L–shaped array (red) and the short circular set-up (black). (b) The two MSPAC dispersion curves obtained using the short (red) and the long (black) L–shaped array.

Table 1. The different inversion processes for different array configurations and dispersion curve analysis method.

Name	ESAC/MSPAC	Configuration
GA1	ESAC	Circle
GA2	ESAC	Long L–shape
NA1	MSPAC	Circle
NA2	ESAC	Long L–shape
NA3	MSPAC	Long L–shape

dispersion curve reflects the characteristics of the layers above the engineering bedrock (Arai and Tokimatsu, 2005).

3.2.3. The shear–wave velocity profiles

The joint inversion process of the H/V and the dispersion curve was performed using two different direct-search algorithms: the Neighbourhood Algorithm (NA) and the Genetic Algorithm (GA). Since similar dispersion curves were obtained for the shorter arrays, only that of the circular array was inverted, along with the dispersion curve of the longer array.

Five different inversions were performed for comparison. These are listed in Table 1, with the name referring to the algorithm used. Since the major parameters which have an effect on the inversion process are the thickness and the V_S of the layers, the other parameters were either left as constants or else left to vary in broad ranges. The limits of V_S were set to 200 m/s and 5000 m/s respectively and it was related to V_S via the Poisson's ratio (a condition only used in the NA), with 0.2 and 0.5 given as limits. The density was kept as a constant of 2000 kg/m^3 to reduce the number of free parameters.

The limits of thickness and V_S were chosen according to known information about the strata and by inspection of the dispersion curve and the geological map of Malta.

The results obtained are displayed in Figures 12 and 13. In general, a very good fit was obtained between the experimental and theoretical dispersion and H/V curves. The final set of best–fitting models also show a very good agreement in the shallow part of the velocity profile (up till around 40 m). The uncertainty however increases with depth, mostly close to and below the bedrock interface, since this part is only

constrained by the H/V curve (Picozzi and Albarello, 2007) which is characterized by a trade–off between the V_S and the thickness. In fact, large uncertainties exist both on the thickness and the velocity scales. From the five best fitting profiles (summary in Table 2), the V_S of the GL at this site can be considered to be around 900–1000 m/s, with only NA1 being an outlier, since a velocity of 750 m/s was obtained. This range is similar to that obtained by Pace (2012) and Panzera *et al.* (2013) in Xemxija and some other sites in Malta. The thickness of the clay obtained for all the models is around 40–50 m. The only model which predicted a 60 m depth to bedrock is GA1. However, one should keep in mind that even though the model with the best misfit is chosen, it is not the only model which gives a low misfit. This highlights the non–uniqueness of the inversion problem. Since in this case, two different inversion algorithms and four distinct dispersion curves were utilized, the results could be compared and a consistent final model could be chosen.

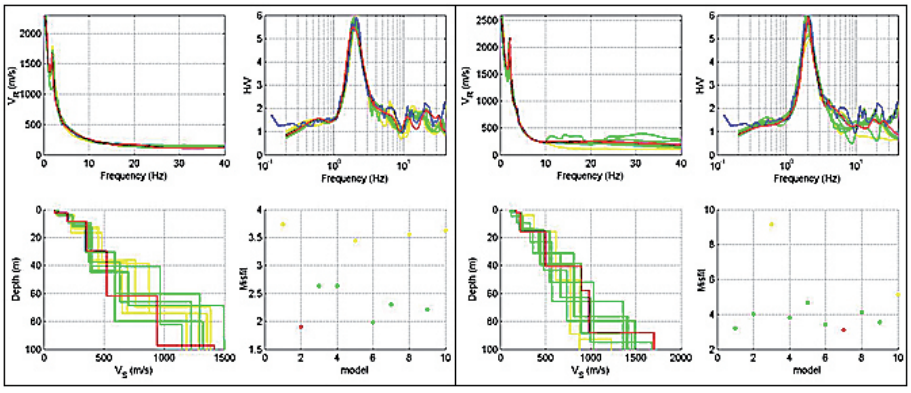

Figure 12. The inversion results for GA1 (left) and GA2 (right). The upper panel graphs show the fitting of the dispersion and H/V curve respectively. The blue curve is the one obtained from the data (i.e. experimental curve), the red curve shows the best fitting theoretical curve (i.e. the one with lowest misfit) while the others (green and yellow) are the curves from the 9 other inversion processes. The profiles in green are those characterised by a misfit which is less than 50 % of the best model's misfit value. The bottom left figure shows the best profile in red along with the profiles from the other runs. The misfits of each of the 10 profiles can be seen in the bottom right figure.

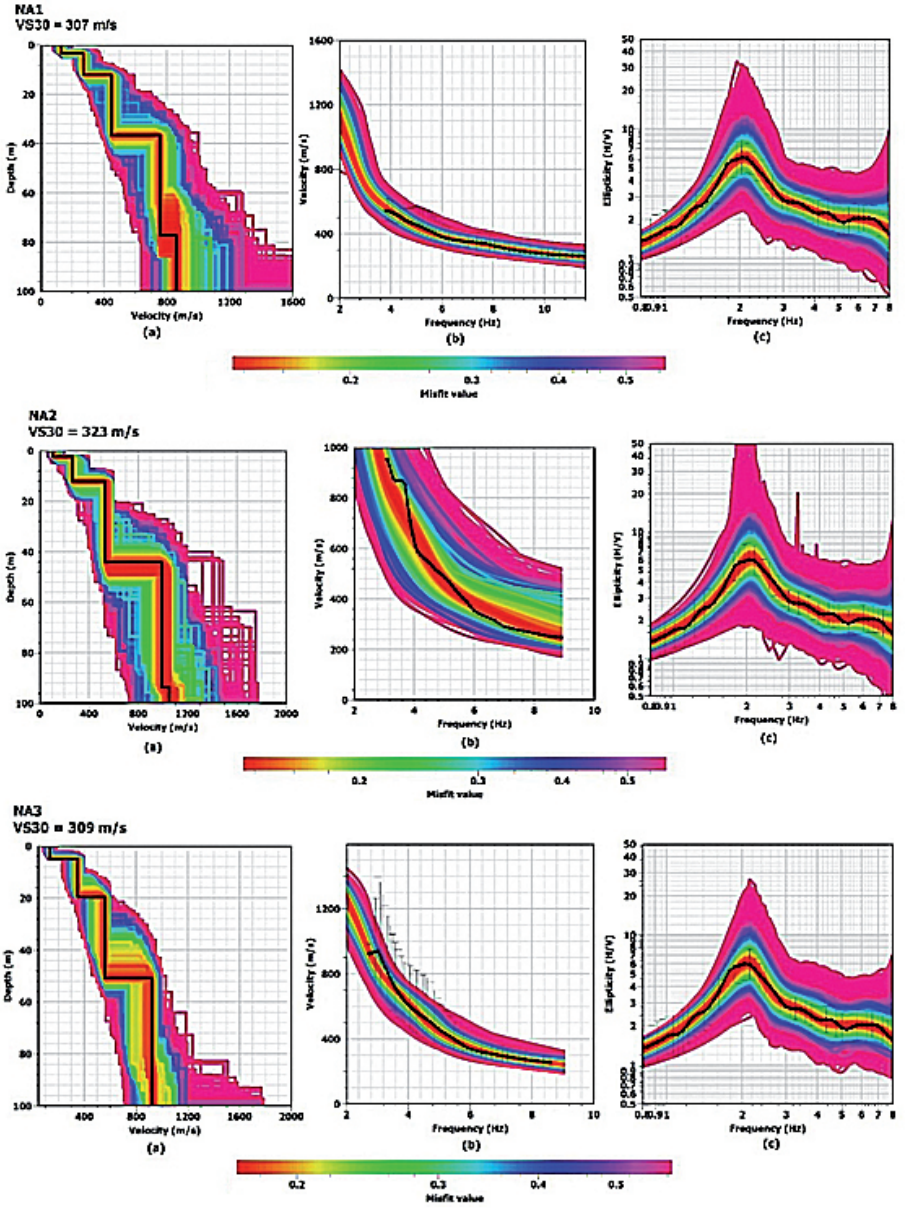

Figure 13. The inversion results for NA1, NA2 and NA3. (a) shows the shear–wave velocity profiles obtained by the joint inversion of the dispersion curve (black curve in (b)) and ellipticity curve (black curve in (c)). The black line in (a) shows the best fitting profile. The colours of the profiles are indicative of the misfit.

Table 2. The final V_S and thickness (H) values obtained for each inversion process for the BC and GL respectively. The thickness of the GL was left out because in this case it was not possible to obtain it due to reasons mentioned in the text.

		BC	GL
GA1	V_S	350 m/s	940 m/s
	H	62 m	n/a
GA2	V_S	325 m/s	900 m/s
	H	40 m	n/a
NA1	V_S	325 m/s	750 m/s
	H	37 m	n/a
NA2	V_S	370 m/s	990 m/s
	H	45 m	n/a
NA3	V_S	375 m/s	925 m/s
	H	51 m	n/a

The calculated V_{S30} values for each profile are 257 m/s, 292 m/s, 307 m/s, 309 m/s and 323 m/s, thus classifying the site as belonging to the class C according to the EC8 classification (Bisch *et al.*, 2012). The average V_S down to bedrock of all the obtained profiles, which can be associated with the BC, was around 350 m/s, which highlights the strong velocity contrasts (factor of 3) between the BC and the GL. This velocity is again in agreement with Pace (2012) and Panzera *et al.* (2013).

4. Acknowledgements

The authors are grateful to Dr. D. Albarello and Dr. E. Lunedei for the use of the ESAC and joint inversion codes. E. Paolucci was supported by Regional PhD Course in Earth Sciences "Pegaso" (Regione Toscana, Italy).

Farrugia D.[1], Paolucci E.[2], D'Amico S.[1], Galea P.[1],
Pace S.[3], Panzera F.[4], Lombardo G.[4] and INGV team[5]

1. Department of Geosciences, University of Malta, Msida MSD2080, Malta. Corresponding author: Farrugia D., dfarrugia28@gmail.com
2. Dipartimento di Scienze Fisiche, della Terra e dell'Ambiente, Università di Siena, Italy.
3. Institute of Earth Systems, University of Malta, Msida MSD2080, Malta.
4. Dipartimento di Scienze Biologiche, Geologiche e Ambientali, Università di Catania, Italy.
5. Istituto Nazionale di Geofisica e Vulcanologia, Sez. Sismologia e Tettonofisica, Roma, Italy.